Robustness of spin polarization against temperature in multilayer structure: Triple quantum well

S. Ullah, F. C. D. Moraes, G. M. Gusev, A. K. Bakarov, and F. G. G. Hernandez

Citation: Journal of Applied Physics **123**, 214306 (2018); doi: 10.1063/1.5022313
View online: https://doi.org/10.1063/1.5022313
View Table of Contents: http://aip.scitation.org/toc/jap/123/21
Published by the American Institute of Physics

Robustness of spin polarization against temperature in multilayer structure: Triple quantum well

S. Ullah,[1,2,a)] F. C. D. Moraes,[1] G. M. Gusev,[1] A. K. Bakarov,[3] and F. G. G. Hernandez[1]
[1]*Instituto de Física, Universidade de São Paulo, Caixa Postal 66318, CEP 05315-970 São Paulo, SP, Brazil*
[2]*Department of Physics, Gomal University, Dera Ismail Khan 29220, KP, Pakistan*
[3]*Institute of Semiconductor Physics and Novosibirsk State University, Novosibirsk 630090, Russia*

(Received 13 January 2018; accepted 15 May 2018; published online 6 June 2018)

We address the temperature influence on the precessional motion of electron spins under a transverse magnetic field, studied in GaAs/AlGaAs triple quantum wells, using pump-probe Kerr rotation. In the presence of an applied in-plane magnetic field, the TRKR measurements show the robustness of carrier's spin polarization against temperature, which can be easily traced in an extended range up to 250 K. By tuning the pump-probe wavelength to the exciton bound to a neutral donor transition, we observed a remarkably long-lasting spin coherence (with dephasing time $T_2^* > 14$ ns) limited by the spin hopping process and exchange interaction between the donor sites, as well as the ensemble spread of the g-factor. The temperature dependent spin dephasing time revealed a double linear dependence due to the different relaxation mechanisms active in respective temperature ranges. We observed that the increase in sample temperature from 5 K to 250 K leads to a strong T_2^* reduction by almost 98%/97% for the excitation wavelengths of 823/821 nm. Furthermore, we noticed that the temperature increase not only causes the reduction of spin lifetime, but can also lead to the variation of the electron g-factor. Additionally, the spin dynamics were studied through the dependencies on the applied magnetic field and optical pump power. *Published by AIP Publishing*. https://doi.org/10.1063/1.5022313

I. INTRODUCTION

Recently, the spin dynamics of carriers and related physics in low-dimensional structures have attracted considerable attention from both viewpoints of physics and its promising applications in spintronic devices.[1–4] Long-lasting spin coherence, persisting up to about room temperature, is one of the key requirements for successful implementation of novel spintronics devices. For that reason, advanced and new material structures exhibiting large spin polarization are highly desirable. A number of efforts have been put forth to enhance the spin lifetime, for example, by using different dimensionally semiconductor nanostructures, such as QWs,[5,6] quantum dots (QDs),[7] and layered structures[8] of various material systems based on III–V [e.g., GaAs, GaN, and (In,Ga)As] and II–VI [e.g., CdTe, ZnSe, and (Zn,Cd)Se] semiconductors.

Based on those efforts, two approaches for the tailoring of carrier spin polarization have emerged. The first relies on the doping of the material, which guarantees the long spin coherence time, while the second is based on the tailoring through the spin-orbit (SO) field. One of those attempts made by the Awschalom group in the bulk[9] and II–VI QW[10] samples, with the doping level close to metal-insulator transition (MIT), was the observation of an extraordinary long coherence time. Those findings, on the one hand, revealed that the long-lived spin coherence is restrained to a doping level in the vicinity of MIT.[11–13] On the other hand, it animated the expectation that the electron spin can be finally realized as a basis for quantum computation. For the device applications, it is highly desirable that the generation and detection of such spin polarization could be carried out at room temperature and a low magnetic field.

While providing a control knob for handling the carrier spins, the spin-orbit coupling (SOC) also leads to an efficient spin relaxation through the Dyakonov-Perel (DP) mechanism.[14] In this mechanism, the random walk of individual spins within the spin-polarized ensemble leads to the random precession of spins around the momentum-dependent internal magnetic field ($\mathbf{B}_{so}$), thus opening a pathway for spin relaxation. By tuning of the sample spin-orbit interaction by changing the sample parameters, one can tailor the electron spin coherence. See, for example, the calculations in Ref. 5 using the sample parameters such as QW width, symmetry, and electron density. However, for the carriers confined within the density of donor states, having zero average wave vectors, the Dyakonov-Perel spin relaxation mechanism does not work. Instead, the randomized magnetic field induced by the SOC leads to the DP like spin relaxation through the spin hopping process between the donor sites or via the exchange interaction between the spin states localized on the adjacent donors.[15]

A number of experimental investigations on the temperature influence of spin dynamics have been carried out in semiconductor QWs;[16,17] however, to our knowledge, none of the reports using multilayer structures have, to date, been appeared in the literature. For the present investigation, we selected the triple quantum well (TQW) because such multilayer structures lead to the discoveries of remarkable phenomena such as the drift of long current-induced spin coherence[18,19] and collapse of the quantum Hall interlayer tunneling gaps.[20] Additionally, such structures also offer possibilities for the generation of spin devices, for example,

a)Author to whom correspondence should be addressed: saeedullah.phy@gmail.com

in the production of spin filters.[21] Despite the fact that in systems with two or more occupied subbands the intra- and intersubband SOC may also suppress the spin coherence, the studied structure shows the robustness of spin polarization against temperature. Remarkably, it results in T_2^* in the nanosecond range for the studied structure with individual subband density beyond the metal-insulator transition.

II. MATERIALS AND EXPERIMENT

The experiments were carried out on a high mobility *n*-GaAs/AlGaAs TQW grown by molecular beam epitaxy (MBE) on a (001)-oriented GaAs substrate. The layered structure of the sample is shown schematically in Fig. 1(a). The sample was remotely δ-doped where three doping layers were deposited into the barrier materials of the quantum wells. The doping layers close to the left and right of the QWs provide carriers for the two-dimensional electron gas (2DEG), while the third doping was carried out to saturate the dangling bonds on the structure. The electrons from the doping layers were being collected into QWs, forming a dense 2DEG with a total electron sheet density of $n_s = 7 \times 10^{11}\,\mathrm{cm}^{-2}$. The sample growth condition was optimized to yield a 22-nm-thick GaAs central well and two 10-nm-thick lateral wells sandwiched between AlGaAs layers. The side wells are separated from the central well by 2-nm-thick $Al_{0.3}Ga_{0.7}As$ barriers. The optimization was found necessary because the electron density mostly concentrates in the side wells as a result of electron repulsion and confinement. The calculated band structure and subband charge density are illustrated in Fig. 1(b), where three subbands, with subband separation of $\Delta_{12} = 1.0\,\mathrm{meV}$, $\Delta_{13} = 3.4\,\mathrm{meV}$, and $\Delta_{23} = 2.4\,\mathrm{meV}$, are formed as a result of interlayer coupling.[22]

The time-resolved Kerr rotation (TRKR) and resonant spin amplification (RSA) techniques were applied to demonstrate the long-lived spin coherence and its robustness against temperature. Both pump and probe pulses were delivered by a Ti-sapphire laser with a pulse duration of 100 fs, operating at a frequency of $f_{rep} = 76\,\mathrm{MHz}$. The polarization of the pump pulse was modulated using a photo-elastic modulator (PEM) operated at 50 kHz for lock-in detection. The circularly polarized pump pulse was focused onto a spot of approximately 50 μm on the sample. For all the experiments, except power dependence, we used the pump power of 1 mW (corresponding to an excitation density of $50\,\mathrm{W/cm}^2$) which gives rise to the photogenerated carrier density of $2.0 \times 10^{11}\,\mathrm{cm}^{-2}$. Varying the time delay Δt between pump and probe pulses, the rotation of the linearly polarized probe upon reflection from the sample surface was recorded using a balanced bridge and double lock-in detection technique.

III. RESULTS AND DISCUSSIONS

A. Magnetic field dependence of spin dynamics

For the selection of right excitation energy, we first measured the TRKR dependence on the laser wavelength. Figure 2(a) shows a series of TRKR traces recorded for different excitation energies with a wavelength ranging from 811 nm to 823 nm, under an applied magnetic field of $B = 1$ T. Obviously, the damping of spin beats and hence T_2^* vary with the laser detuning when occupying the conduction and donor band states. The magneto-photoluminescence spectra of the studied structure can be found in Ref. 20, where two distinct regions were pointed out. The region at low wavelengths was correlated with the direct recombination between the states confined in the conduction and valence bands, where the one at high wavelengths was associated with an exciton

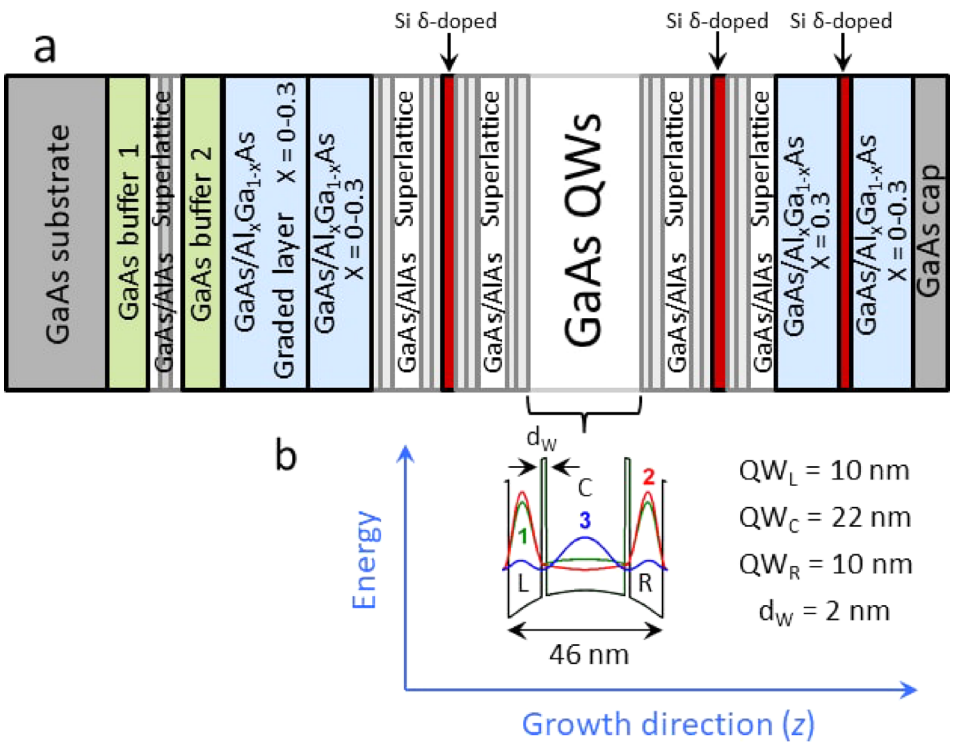

FIG. 1. (a) Schematic layer structure of the triple quantum well grown by MBE along $\hat{z} \parallel [001]$. (b) TQW band structure and charge density for the three occupied subbands with subband separation $\Delta_{12} = 1.0\,\mathrm{meV}$, $\Delta_{23} = 2.4\,\mathrm{meV}$, and $\Delta_{13} = 3.4\,\mathrm{meV}$.

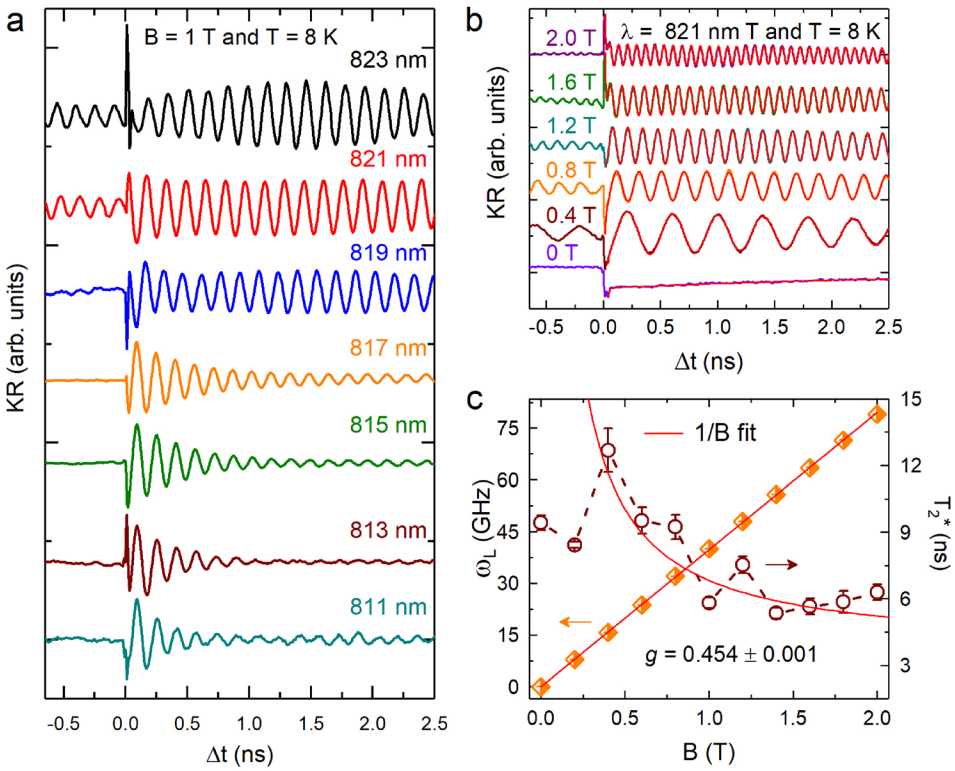

FIG. 2. (a) KR as a function of pump-probe delay measured for different wavelengths. (b) Fit to the Kerr rotation of optically induced spin polarization for various magnetic fields. (c) T_2^* and ω_L as a function of the applied magnetic field where solid red lines are fit to the data.

bound to a neutral donor (DX center). For the conduction band states (low wavelengths), T_2^* is smaller, whereas for higher wavelengths, at which the donor states are pumped, T_2^* is much longer and persists between successive pulses as evidenced by the non-vanishing signal at $\Delta t < 0$. Our data are in agreement with a similar study reported in *n*-type bulk GaAs doped beyond MIT, where a strong variation of T_2^*, about three order of magnitude, as a function of excitation energy, was found when occupying donor and conduction band states.[23] For the robustness of spin polarization, we chose the DX transition energies as these energies yield long-lasting spin signals. Additionally, for $\lambda = 823$ nm, one can clearly see that the KR amplitude increases with time delay. In spatially resolved Kerr rotation, such a behavior was attributed to the out-diffusion of photo-generated spins from the region of the laser spot.[24] However, in the present case, such a contribution was restricted by increasing the size of the spot to 50 μm. In our experiment, such an effect originates due to the anti-phase contribution from the previous pulse.

Figure 2(b) shows the time evolution of Kerr rotation recorded with and without an external magnetic field up to 2 T applied along x, i.e., in the Voigt geometry. TRKR traces (measured at $T = 8$ K and $\lambda = 821$ nm) show periodic oscillation in the external magnetic field, denoting the existence of spin signals. These oscillations result from the spin precession around the applied in-plane magnetic field with a beating frequency (ω_L). Increasing the magnitude of the applied magnetic field speeds up the precessional frequency as evidenced from the TRKR traces. Furthermore, the decay of spin beat amplitude is very slow lasting more than the period of laser pulses ($t_{rep} = 13.2$ ns).

The measured TRKR signals are well described by the following function:

$$\Theta_K = A \exp\left(\frac{-\Delta t}{T_2^*}\right) \cos(\omega_L \Delta t + \phi) + y_0, \qquad (1)$$

where A is the initial spin polarization amplitude, Δt is the time delay between the pump and probe pulses, T_2^* is the ensemble dephasing time, ϕ is the initial phase, y_0 is the Kerr signal offset, and $\omega_L = |g|\mu_B B/\hbar$ is the Larmor precession frequency with electron g-factor $|g|$, Bohr magneton μ_B, magnetic field B, and reduced Planck's constant $\hbar$. The experimental curves were fitted to an exponential decay function for $B = 0$ and an exponentially decaying cosine function [Eq. (1)] for $B \neq 0$ as shown by red curves plotted on the top of experimental data. ω_L (for $B \neq 0$) and T_2^* retrieved from the fit are displayed in Fig. 2(c). As expected, ω_L varies linearly with an applied magnetic field which is typical for the electrons;[5,18] however, for holes, non-linearities can occur due to band mixing as reported for GaAs/$In_xGa_{1-x}As$ QWs.[25] The slope (solid red line) yields a g-factor (absolute value) of $g = 0.454 \pm 0.001$, where its comparison with the bulk $|g|$ value further supports that the observed signals correspond to electron carriers.

The spin dephasing time varies with the growing magnetic field [see, for example, Fig. 2(c)]. T_2^* first increases to a maximum value of ~12.7 ns at $B = 0.4$ T and then decreases with a further increase in the magnetic field due to the spread in the ensemble g-factor.[5,26] The observed increase may be caused by the cyclotron motion acting as a momentum scattering, which in agreement with the Dyakonov-Perel mechanism leads to a less efficient spin relaxation.[14] The reduction of T_2^* with a magnetic field follows the 1/B dependence,

where the size of inhomogeneity can be inferred from the linear dependence of the relaxation rate on the applied magnetic field, $1/T_2^* = \Delta g \mu_B B/2\hbar$.[26] We evaluated $\Delta g = 0.0005$, which is only 0.11% of the observed g-factor, suggesting that the spread of the ensemble g-factor is not the only mechanism responsible for the spin relaxation. However, in QDs, Δg can be quite sizable and can result in an efficient dephasing.

B. Temperature influence on spin dynamics while tuning laser energy to donor states

A representative selection of TRKR traces measured for various temperatures in the range from 5 K to 250 K is shown in Fig. 3(a). For clarity of presentation, the TRKR traces are vertically shifted, and the curves at higher temperature are upscaled by multiplying with indicated numbers labeled inside the panel. To highlight the trends at negative Δt, the curves are normalized to the time origin ($\Delta t = 0$). One can clearly see significant changes in the carrier spin precession with rising temperature as highlighted by vertical dashed lines. The precession frequency slows down with increasing temperature, and the decay of spin beat amplitude is thermally stimulated. Additionally, the curves at low temperature (5–50 K) look phase shifted by Π with respect to 140 and 250 K curves due to the generation of initial spin polarization in the opposite directions. This phase shift may be possibly due to the contribution of hole spin polarization to that of the electrons in the initial few picoseconds. Such a shift can also be seen in the magnetic field dependence where the hole contribution is evidenced by the shift of the center of gravity of the carrier spin precession.

Also, at low temperatures in the range from 5 K to 35 K, the electron spin beating at positive delays is accompanied by spin beating even at negative delays due to the long-lived spin coherence persisting between successive pulses. In such cases, the spin dephasing time in excess of t_{rep} can be retrieved by using the RSA technique.[9]

Figure 3(b) displays the RSA pattern recorded at $\Delta t = -0.24$ ns while sweeping the magnetic field over a range of −200 mT to 200 mT. We observed sharp resonance peaks with spacing ΔB corresponding to the spin precession frequencies which are commensurable with the pulse repetition period obeying the periodic condition $\Delta B = h/g\mu_B t_{rep}$.[9] T_2^* can be directly evaluated from the width of those peaks using the Lorentzian model

$$\Theta_K = A \Big/ \left[(\omega_L T_2^*)^2 + 1\right], \tag{2}$$

where the half-width $B_{1/2}$ of RSA peaks points to the spin dephasing time $T_2^* = \hbar/g\mu_B B_{1/2}$. From the RSA spectrum, the following significant features can be directly extracted. First, in the temperature range from 5 K to 20 K, the RSA peaks centered at $B = 0$ are smaller in amplitude than the peaks at $B \neq 0$. The depression of these zeroth-field resonant peaks is due to the spin relaxation anisotropy[27,28] caused by an internal magnetic field. The direction and magnitude of this internal field can be obtained by fitting the data to the model formulated in Ref. 29, for example, as shown in Fig. 3(b) by red curves (in a selective range from −100 to 100 mT) for $T = 15$ K. The fitting yields the magnitude of the internal magnetic field $B_\perp = 0.0017$ mT which causes spin relaxation in the material. A more detailed analysis of anisotropic spin relaxation, the internal magnetic field, and its influence on experimental parameters is published in Ref. 30.

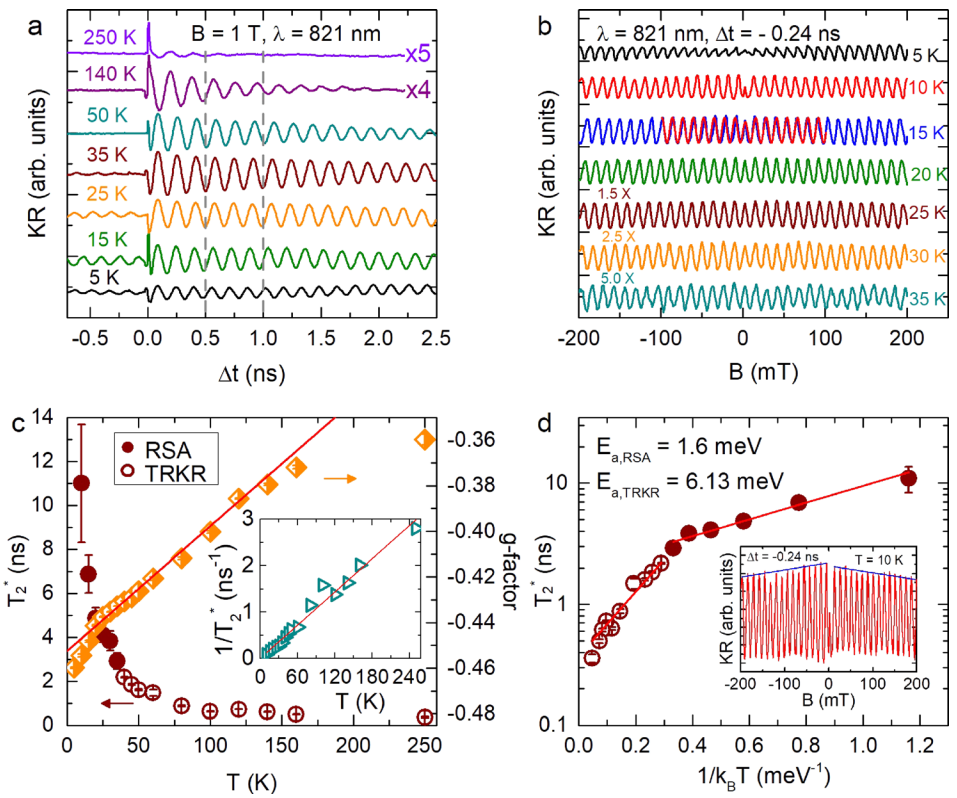

FIG. 3. Temperature influence on spin dynamics. (a) Spin precession measured at various temperatures in the range from 5 K to 250 K. (b) RSA measured at $\Delta t = -0.24$ ns for different temperatures. (c) The electron g-factor and T_2^* extracted from the RSA (solid circles) and TRKR (open circles) as a function of temperature. The solid red line is a linear fit to the data. The size of error bars shows the uncertainty in the measured values. The inset shows the temperature dependence of the spin relaxation rate with linear interpolation (red line). (d) T_2^* as a function of $1/k_BT$ fitted to the Arrhenius-like function (solid lines). The measurement parameters are listed inside the corresponding panels. The inset in Fig. 3(d) highlights the decrease in the amplitude of finite field RSA peaks with the increasing magnetic field.

Second, the data support a transition from anisotropic to isotropic spin relaxation with growing temperature, i.e., with the rise of temperature, the amplitude of the peak centered at $B = 0$ increases and becomes equal to that of finite field peaks at a higher temperature. Third, the amplitude of the finite field RSA peaks decreases with the increasing magnetic field due to the ensemble spread of the electron g-factor as noted above. However, plotting a series of RSA curves may be hiding this trend. See, for example, the RSA curve [inset of Fig. 3(d)] recorded at $T = 10$ K where the trend is clearly visible. Fourth, at $T = 5$ K, the resonant peaks have larger amplitude at a higher magnetic field which is a well-known indication of the long hole spin coherence time involved in the generation of spin coherence time.[31]

T_2^* received from the Lorentzian fit to the RSA peaks is depicted in Fig. 3(c) by closed circles together with the data points extracted from TRKR (open circles). The TRKR signal recorded at $T = 250$ K showed a biphasic spin dynamics and was fitted to Eq. (1) plus a non-oscillatory exponential decay to account for the fast decay over first few picoseconds. The fitting yields decay times with $T_{2_1}^* = 8.5$ ps (corresponding to the hole spin dynamics) and a relatively long $T_{2_2}^* = 0.357$ ns (related to the electron spin dynamics). In the studied temperature range, $5\,\text{K} < T < 250\,\text{K}$, the electron g-factor increases from -0.46 to -0.36 [see Fig. 3(c)]. For the temperature up to 160 K, a good linear dependence on temperature, $g(\text{T}) = -0.452 + 5.37 \times 10^{-4}\,T$, was observed. Our findings are in good agreement with a similar investigation reported on bulk GaAs.[32,33] In Ref. 32, the experimentally observed g-factor was approximated by $g(\text{T}) = -0.44 + 5.0 \times 10^{-4} T$ for a temperature ranged from liquid helium temperature up to room temperature.

We observed a strong T_2^* reduction with temperature, decreasing down to 0.36 ns at $T = 250$ K. T_2^* versus temperature shows a double linear dependence which is even more pronounced when dephasing time is plotted as a function of reciprocal thermal energy ($1/k_BT$). The observed dependence was attributed to the different spin relaxation mechanisms active in respective temperature ranges. At low temperatures, the spin relaxation was caused by an exchange interaction with other localized donor states. However, at high temperatures, the spin relaxation was governed by a carrier hopping process between the nearby donor sites.[12] In the presence of a randomized spin-orbit field, both the exchange interaction between the spin states localized on the adjacent donors and the spin hopping process may lead to the change in electron spin states. Therefore, in principle, they can result in the spin relaxation. These processes can lead to a linear increase in the spin dephasing rate ($1/T_2^*$), in a similar way as for the classical DP mechanism, with temperature. Such a linear increase in the relaxation rate, received from the TRKR and RSA, is shown in the inset of Fig. 3(c). Figure 3(d) shows the relaxation times as a function of reciprocal thermal energy fitted to the Arrhenius law: $A\exp(E_a/k_BT)$, where A is the Arrhenius free-exponential factor, E_a is the activation energy, and k_B is the Boltzmann constant. The fit to the data yields the activation energies, labeled inside the corresponding panel, which are attributed to the hopping process between the donor sites.

Concerning the subband dependence of spin dynamics, the laser energy was changed by about 3 meV ($\simeq \Delta_{13}$) by increasing the pump-probe wavelength from 821 to 823 nm. Figure 4(a) shows a set of TRKR traces measured at different temperatures while tuning the laser wavelength to 823 nm and keeping the experimental conditions the same as were

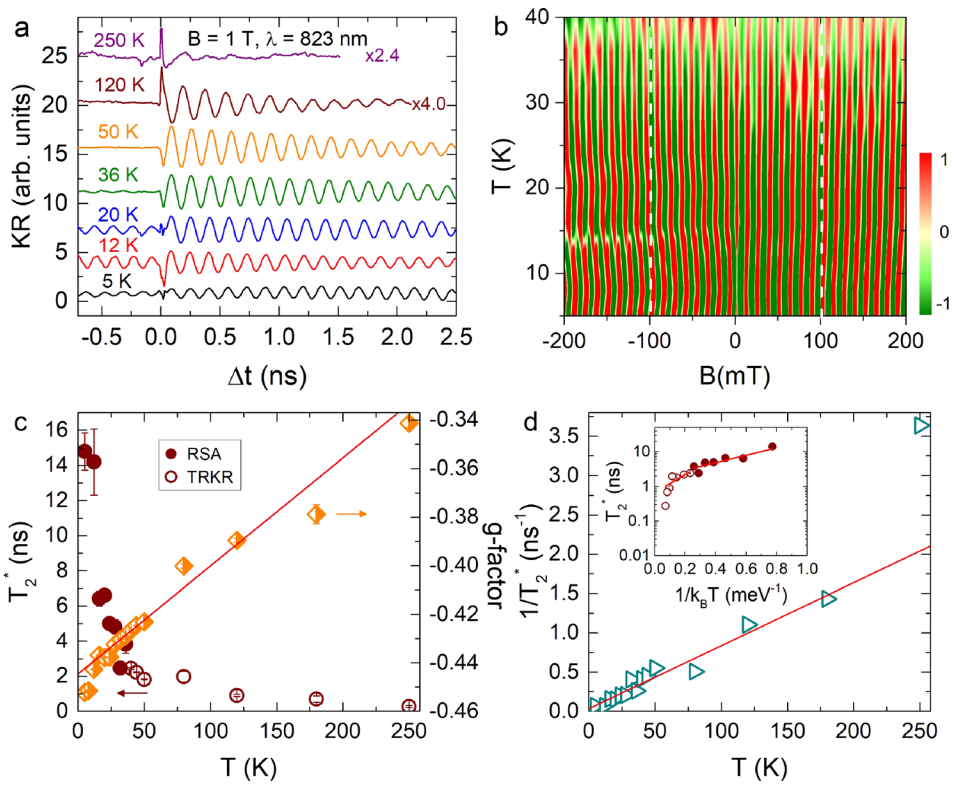

FIG. 4. Temperature influence on spin dynamics. (a) KR vs Δt recorded at different temperatures. (b) Temperature dependence of resonant spin amplification. (c) The g-factor and T_2^* as a function of sample temperature where T_2^* retrieved from the RSA signal is shown by solid circles, while open circles depict the one obtained from the TRKR. (d) Temperature dependence of $1/T_2^*$ with a linear fit to the data (red line). The inset shows T_2^* as a function of reciprocal thermal energy fitted to the Arrhenius-like function.

used in the previous figures (Figs. 2 and 3) for a maximum KR signal. One can clearly see that the precession frequency gets smaller with growing temperature which directly affects the electron g-factor through the relationship described in Sec. III A. As shown, all the data except the ones at elevated temperatures show a single exponential decay. However, for the present study, only the spin relaxation of electrons is concerned, while the short relaxation times (such as hole spin polarization) are disregarded. The pronounced oscillation at negative time delays, of the amplitude comparable to the one at positive delays, observed at low temperatures suggests that $T_2^* \geq t_{rep}$.

In analogy to the previous discussion, we used the RSA technique[9] to extract T_2^*, which takes into account the constructive interference of the coherent spin oscillations from successive pulses. Such an RSA pattern measured at $\Delta t = -0.24$ ns is shown in Fig. 3(b). The superposition of spins that were created by the pulse train 13.2 ns before the arrival of the next pulse causes a series of sharp resonance peaks as revealed by a striped pattern. The rise of temperature accelerates the decay of spin polarization due to heating, and the RSA peaks disappear into noise (white shades) at higher temperature (see, for example, the peaks at $T \geq 35$ K). Additionally, the variation of the g-factor is clearly evidenced by the change in the spacing, ΔB, between RSA peaks. That is with growing temperature, the outer peaks shift toward higher magnetic fields as marked by white dashed lines at $B = \pm 100$ mT.

The electron g-factor, received from the TRKR oscillation, increases linearly with a slope of 4.87×10^{-4} K^{-1}. Again, the present findings are in agreement with the literature results.[32,33] T_2^* extracted from the RSA (solid circles) and TRKR (open circles), plotted in Fig. 4(c), shows a strong reduction with temperature. Figure 4(d) shows the temperature dependence of $1/T_2^*$ following a linear increase, up to 190 K, with a slope of 0.008 ns^{-1} K^{-1}. The trends of shortening T_2^* above 190 K, deviating from the linear behavior, suggest that the higher temperature causes the heating effect, which leads to low spin polarization as commented above. The inset shows T_2^* as a function of $1/k_BT$, fitted to the Arrhenius-like function, yielding activation energies of 2.43 meV and 6.01 meV for the RSA and TRKR, respectively. The difference in T_2^*, while changing the laser energy by about 3 meV ($\simeq \Delta_{13}$), may be associated with the relative different charge density distribution of electrons in the first and third subbands.

C. Dependence of spin dynamics on optical power

In this section, we report on the excitation power influence on the spin dynamics measured using time-resolved Kerr rotation. Figure 5(a) shows the pump-probe delay scans of the KR signal measured, at $B = 1$ T applied normal to the initial spin polarization, for different excitation powers in the range from 1 mW to 7 mW (corresponding to 50–350 W/cm^2). At a low pump power of 1 mW, the density of photogenerated carriers is comparable to the 2DEG density; however, at high power, the photogenerated density exceeds the density of 2DEG by an order of magnitude. The striking feature of the KR traces is the appearance of a long-lived spin beating as can be seen at negative time delay. The electron g-factor evaluated from the fit of experimental data is shown in Fig. 5(b). As expected we did not see any influence of the optical pump power on the g-factor which is directly reflected from the constant spin beat frequency marked by dotted lines in panel (a).

The resulted values of T_2^*, plotted in Fig. 5(c), remain constant in the low power range. However, a further increase in excitation power results in the decrease in T_2^*. For the single QW structure, the reduction of T_2^* at high pump density was assigned to the heating effect induced by optical

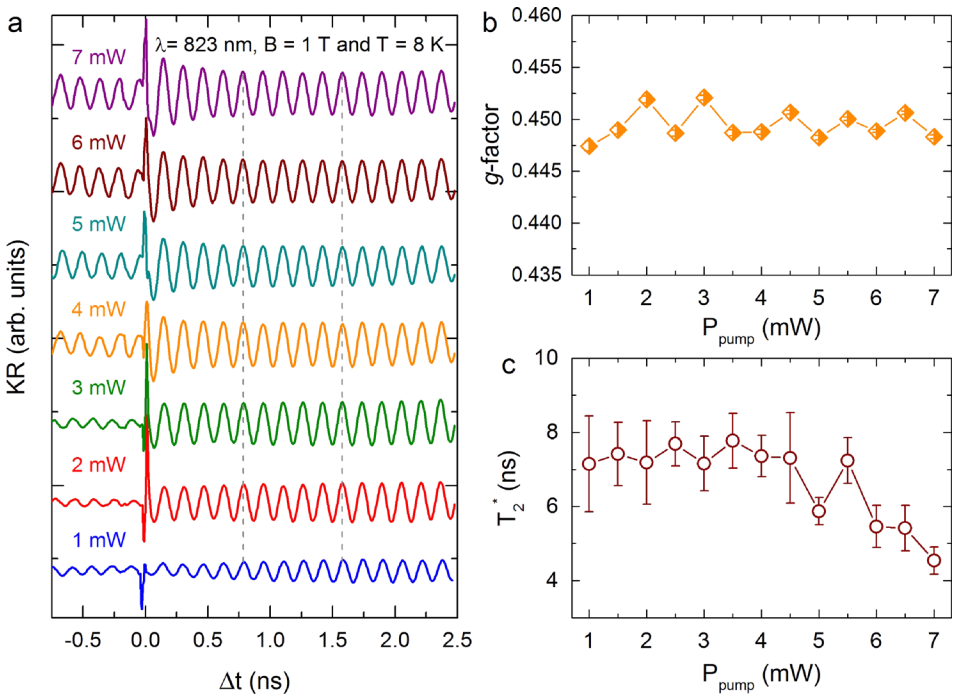

FIG. 5. Pump power influence on the spin dynamics: (a) TRKR signals as a function of excitation power. The evaluated (b) g-factor and (c) T_2^* as a function of pump power. The measurement parameters are listed in (a).

excitation.[34] In our structure, we attribute this decrease to an increased efficiency of the Bir-Aronov-Pikus (BAP) mechanism induced by the high density of photogenerated carriers. As a key factor for practical spintronics, we noticed that T_2^* still remains in the nanosecond range when the excitation power is raised by almost one order of magnitude. The observed long-lasting T_2^* results from the simultaneous suppression of BAP and spin-orbit relaxation mechanisms governed by spin hopping and exchange between adjacent donor sites.

IV. CONCLUSIONS

In summary, we have studied the magnetic field, sample temperature, and optical pump power dependence of spin dynamics in GaAs/AlGaAs triple quantum wells using pump-probe Kerr rotation. It has been found that the spin polarization in our sample is robust against temperature and was apparent up to $T = 250\,\mathrm{K}$. The increase in excitation energy about 3 meV ($\simeq \Delta_{13}$), by varying the laser wavelength from 823 nm to 821 nm, causes a T_2^* reduction of 25% at $T = 250\,\mathrm{K}$. The spin-orbit relaxation powered by the spin hopping process or the exchange interaction between the states localized on nearby donors leads to a linear increase in the dephasing rate on temperature. Additionally, the electron g-factor was also noticed to be varying linearly with temperature. This behavior is in agreement with the data reported on bulk GaAs.[32,33] The present results that are the observed long-lived spin coherence persisting up to high temperature, and the spin relaxation anisotropy, highlights the attractiveness of multilayer structure for practical spintronics.

ACKNOWLEDGMENTS

F.G.G.H. acknowledges the financial support from Grant Nos. 2009/15007-5, 2013/03450-7, 2014/25981-7, and 2015/16191-5 of the São Paulo Research Foundation (FAPESP). S.U. thanks TWAS/CNPq for financial support.

[1]M. I. Dyakonov, "Springer Series in Solid-State Sciences," in *Spin Physics in Semiconductors* (Springer, Berlin, Heidelberg, 2010).
[2]D. D. Awschalom, D. Loss, and N. Samarth, *Semiconductor Spintronics and Quantum Computation* (Springer Science + Business Media, 2013).
[3]I. Žutić, J. Fabian, and S. D. Sarma, Rev. Mod. Phys. **76**, 323 (2004).
[4]J. Fabian, A. Matos-Abiague, C. Ertler, P. Stano, and I. Žutić, Acta Phys. Slovaca **57**, 565 (2007).
[5]S. Ullah, G. M. Gusev, A. K. Bakarov, and F. G. G. Hernandez, J. Appl. Phys. **119**, 215701 (2016).
[6]V. Sih and D. D. Awschalom, J. Appl. Phys. **101**, 081710 (2007).
[7]D. H. Feng, X. Li, T. Q. Jia, X. Q. Pan, Z. R. Sun, and Z. Z. Xu, Appl. Phys. Lett. **100**, 122406 (2012).
[8]J. Berezovsky, O. Gywat, F. Meier, D. Battaglia, X. Peng, and D. D. Awschalom, Nat. Phys. **2**, 831 (2006).
[9]J. M. Kikkawa and D. D. Awschalom, Phys. Rev. Lett. **80**, 4313 (1998).
[10]J. M. Kikkawa, I. P. Smorchkova, N. Samarth, and D. D. Awschalom, Science **277**, 1284 (1997).
[11]R. I. Dzhioev, K. V. Kavokin, V. L. Korenev, M. V. Lazarev, B. Y. Meltser, M. N. Stepanova, B. P. Zakharchenya, D. Gammon, and D. S. Katzer, Phys. Rev. B **66**, 245204 (2002).
[12]M. Römer, H. Bernien, G. Müller, D. Schuh, J. Hübner, and M. Oestreich, Phys. Rev. B **81**, 075216 (2010).
[13]J. S. Sandhu, A. P. Heberle, J. J. Baumberg, and J. R. A. Cleaver, Phys. Rev. Lett. **86**, 2150 (2001).
[14]M. I. Dyakonov and V. I. Perel, Sov. J. Exp. Theor. Phys. **33**, 1053 (1971).
[15]K. V. Kavokin, Semicond. Sci. Technol. **23**, 114009 (2008).
[16]A. Malinowski, R. S. Britton, T. Grevatt, R. T. Harley, D. A. Ritchie, and M. Y. Simmons, Phys. Rev. B **62**, 13034 (2000).
[17]Y. Ohno, R. Terauchi, T. Adachi, F. Matsukura, and H. Ohno, Phys. Rev. Lett. **83**, 4196 (1999).
[18]F. G. G. Hernandez, S. Ullah, G. J. Ferreira, N. M. Kawahala, G. M. Gusev, and A. K. Bakarov, Phys. Rev. B **94**, 045305 (2016).
[19]S. Ullah, G. J. Ferreira, G. M. Gusev, A. K. Bakarov, and F. G. G. Hernandez, J. Phys.: Conf. Ser. **864**, 012060 (2017).
[20]L. F. dos Santos, B. G. Barbosa, G. M. Gusev, J. Ludwig, D. Smirnov, A. K. Bakarov, and Y. A. Pusep, Phys. Rev. B **89**, 195113 (2014).
[21]H. Cruz and D. Luiz, J. Appl. Phys. **104**, 083715 (2008).
[22]S. Wiedmann, N. C. Mamani, G. M. Gusev, O. E. Raichev, A. K. Bakarov, and J. C. Portal, Phys. Rev. B **80**, 245306 (2009).
[23]L. Schreiber, M. Heidkamp, T. Rohleder, B. Beschoten, and G. Güntherodt, preprint arXiv:0706.1884 (2007).
[24]L. Nádvorník, P. Němec, T. Jsnda, K. Olejník, V. Novák, V. Skoromets, H. Němec, P. Kuěel, F. Trojánek, T. Jungwirth *et al*., Sci. Rep. **6**, 22901 (2016).
[25]N. J. Traynor, R. T. Harley, and R. J. Warburton, Phys. Rev. B **51**, 7361 (1995).
[26]E. A. Zhukov, D. R. Yakovlev, M. Bayer, G. Karczewski, T. Wojtowicz, and J. Kossut, Phys. Status Solidi (b) **243**, 878 (2006).
[27]M. M. Glazov and E. L. Ivchenko, Semiconductors **42**, 951 (2008).
[28]I. A. Yugova, M. M. Glazov, D. R. Yakovlev, A. A. Sokolova, and M. Bayer, Phys. Rev. B **85**, 125304 (2012).
[29]B. M. Norman, C. J. Trowbridge, D. D. Awschalom, and V. Sih, Phys. Rev. Lett. **112**, 056601 (2014).
[30]S. Ullah, G. M. Gusev, A. K. Bakarov, and F. G. G. Hernandez, J. Appl. Phys. **121**, 205703 (2017).
[31]I. A. Yugova, A. A. Sokolova, D. R. Yakovlev, A. Greilich, D. Reuter, A. D. Wieck, and M. Bayer, Phys. Rev. Lett. **102**, 167402 (2009).
[32]M. Oestreich, S. Hallstein, A. P. Heberle, K. Eberl, E. Bauser, and W. W. Rühle, Phys. Rev. B **53**, 7911 (1996).
[33]W. Zawadzki, P. Pfeffer, R. Brastchitsch, Z. Chen, S. T. Cundiff, B. N. Murdin, and C. R. Pidgeon, Phys. Rev. B **78**, 245203 (2008).
[34]E. A. Zhukov, D. R. Yakovlev, M. Bayer, M. M. Glazov, E. L. Ivchenko, G. Karczewski, T. Wojtowicz, and J. Kossut, Phys. Rev. B **76**, 205310 (2007).